Canadian Mineralogist
Vol. 30, pp. 1143-1152 (1992)

BARIAN FELDSPAR AND MUSCOVITE FROM THE KIPUSHI Zn–Pb–Cu DEPOSIT, SHABA, ZAIRE

MUMBA CHABU
Laboratoire de Métallogénie, Université de Lubumbashi, B.P. 1825, Lubumbashi, Zaïre

JACQUES BOULÈGUE
Laboratoire de Géochimie et Métallogénie, Université Pierre et Marie Curie, Paris VI, Tour 16–26, 4, Place Jussieu, 75252 Paris Cedex 05, France

Abstract

Barian-bearing feldspar and muscovite are associated with barite in the sulfide mineralization of the Kipushi Zn–Pb–Cu deposit (Zaire), hosted by Lower Kundelungu dolomites and dolomitic shales, in part brecciated, of Late Proterozoic age. The celsian (Cn) content of (Ba,K)-feldspars, which include celsian, hyalophane and orthoclase, varies from 1 to 84 mole %, but exhibits two discontinuities, at Cn_{5-30} and Cn_{40-50}. The coexisting albite is mostly barium-free. The highest BaO content measured in muscovite is 7.66 wt.%, but values around 6 wt.% BaO are more common, even though the associated feldspars vary from Ba-bearing orthoclase to celsian. The replacement of K by Ba in muscovite follows the substitution BaAl = (K,Na)Si and is accompanied by increasing vacancies in octahedral positions and by the replacement of Al by Ti. The muscovite also is phengitic, showing the exchange $(Mg,Fe)^{2+}Si^{4+} = {}^{VI}Al^{IV}Al$. Structural and textural fabrics indicate that Katangan regional metamorphism postdated the mineralization. It is characterized by mineral assemblages of the greenschist facies. We contend that barian muscovite and (Ba,K)-feldspar are metamorphic in origin, and that their barium content was inherited from barite associated with the Zn–Pb–Cu ores.

Keywords: barian feldspar, barian muscovite, barite, Kipushi Zn–Pb–Cu deposit, Lower Kundelungu Group, celsian, hyalophane, orthoclase, substitution schemes, Katangan metamorphism, Zaire.

Sommaire

Des exemples de feldspath et de muscovite baryfères sont associés à la barytine dans les minerais sulfurés du gisement Zn–Pb–Cu de Kipushi (Zaïre), encaissé dans les dolomies et shales dolomitiques, en partie bréchifiés, du groupe du Kundelungu inférieur, d'âge protérozoïque supérieur. La teneur en celsiane du feldspath varie de 1 à 84% (base molaire), mais elle présente une discontinuité majeure entre Cn_5 et Cn_{30}, et une autre moins marquée entre Cn_{40} et Cn_{50}. L'albite associée renferme très peu ou pas de Ba. La muscovite la plus riche en Ba contient jusqu'à 7.66% BaO en poids, mais les valeurs autour de 6% sont plus courantes quelle que soit la nature du felspath baryfère associé. Le remplacement du K par le Ba dans le réseau de la muscovite obéit à la substitution BaAl = KSi accompagnée de lacunes dans les sites octahédriques et par le remplacement de Al par Ti. Une substitution phengitique est également observée dans ce mica. Des données structurales et texturales indiquent que le métamorphisme régional katanguien est postérieur à la mise en place de la minéralisation. Nous considérons que la muscovite et le feldspath baryfères sont d'origine métamorphique et que le baryum qu'ils contiennent a été hérité de la barytine associée au minerai.

Mots-clés: feldspath baryfère, muscovite baryfère, barytine, gisement Zn–Pb–Cu de Kipushi, Kundelungu inférieur, celsiane, hyalophane, orthose, modèle de substitution, métamorphisme régional katanguien, Zaïre.

Introduction

The Kipushi deposit is one of three major carbonate-hosted Zn–Pb deposits that have been recognized in Shaba province, southeastern Zaire. They all occur at the same stratigraphic level, in the Lower Kundelungu Group, just as the Kabwe lead–zinc deposit of Zambia, whereas the Cu–Co and U–(Ni–Co) deposits are found in a lower stratigraphic position, in the Roan Super-group, in both Zambia and Zaire; the Zambian deposits are stratigraphically below their Zairean counterparts (Lefebvre & Tshiauka 1986).

In the Kipushi deposit, the gangue contains (Ba,K)-feldspars including celsian, hyalophane and orthoclase. These occur in association with barian muscovite and barite as accessory minerals within the ore zones, along with quartz, chlorite and dolomite.

Barian silicates are rare and most commonly occur in

manganese deposits (Deer *et al.* 1962, 1963). Very few compositions have been reported in the literature. In this study, we provide analytical data for (Ba,K)-feldspar and barian muscovite resulting from the metamorphism of a carbonate-hosted base-metal deposit. Coupled substitution of Ba for K and Al for Si is characteristic of both muscovite and feldspar.

Geological Setting

The Kipushi deposit has been studied by Intiomale & Oosterbosch (1974), Intiomale (1982), de Magnée & François (1988) and Chabu (1990), who described the geology and tectonic setting of the area. The deposit is one of over 35 occurrences of Cu–Co, U–(Ni–Co) and Zn–Pb deposits that together constitute the Central African Copperbelt of Zaire and Zambia, a region that contains about 15% of world's copper reserves.

Deposits in the Copperbelt are hosted by Late Proterozoic Katangan sediments exposed in the Lufilian fold belt (Fig. 1). The sediments were deformed during the Katangan (also known as Lufilian) Pan-African orogeny (*ca.* 650–500 Ma) and thrust to the north. The Katangan sequence consists of conglomerates, arkoses, greywackes, sandstones, shales, carbonates, and of two tillitic formations totalling nearly 10,000 m in thickness. It is subdivided, from bottom to top, into the Roan and Kundelungu Supergroups. The base of the latter is marked by a tillite, the "Grand Conglomérat", which represents a lithostratigraphic marker of regional extent. The other tillite of the Katangan sequence, the "Petit Conglomérat", divides the Kundelungu Supergroup into the Lower Kundelungu and the Upper Kundelungu Groups (Fig. 2). In the Zairean Copperbelt, rocks of the Roan Supergroup invariably appear as huge fragments up to several kilometers wide, in megabreccias located in the cores of anticlines. Because of that fact, its base is unknown.

The Kipushi Zn–Pb–Cu deposit is located on the northern flank of the Kipushi anticline (Fig. 3), near the contact between a complex breccia field with rocks of the Lower Kundelungu Group. The eastern limit of the

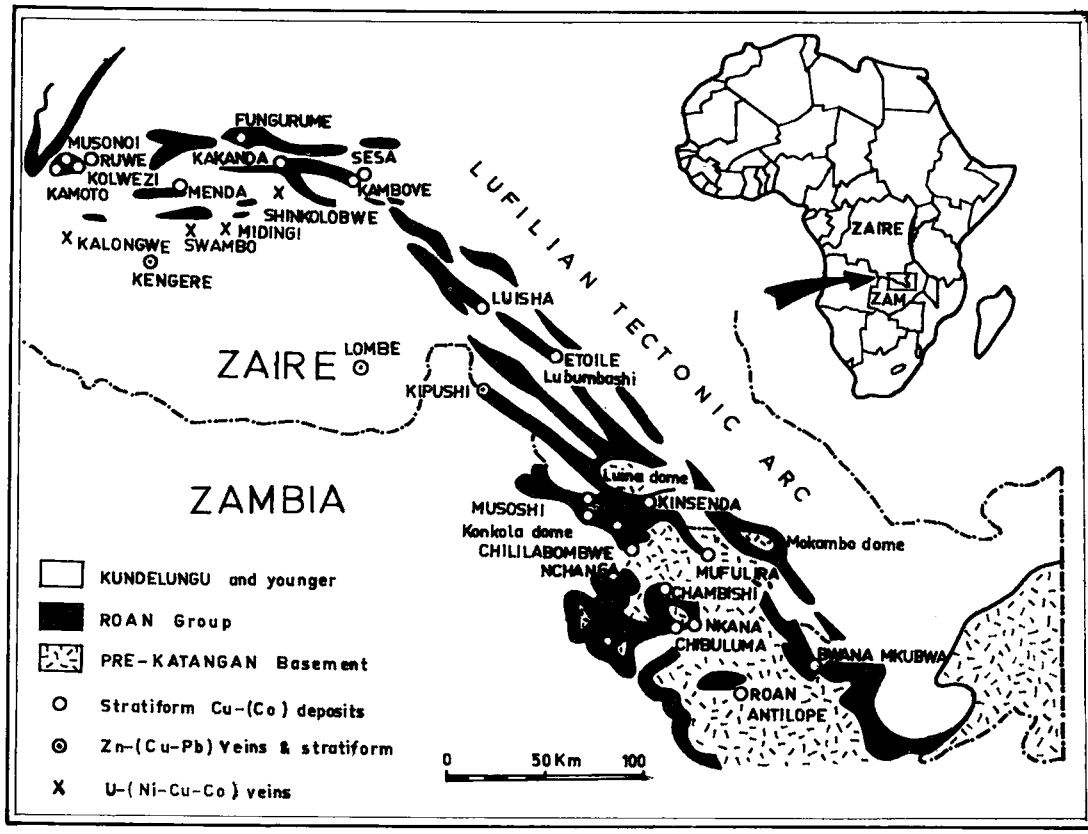

FIG. 1. Simplified geological map of the Lufilian fold belt showing the locations of major deposits. Modified after Sodimiza Company records.

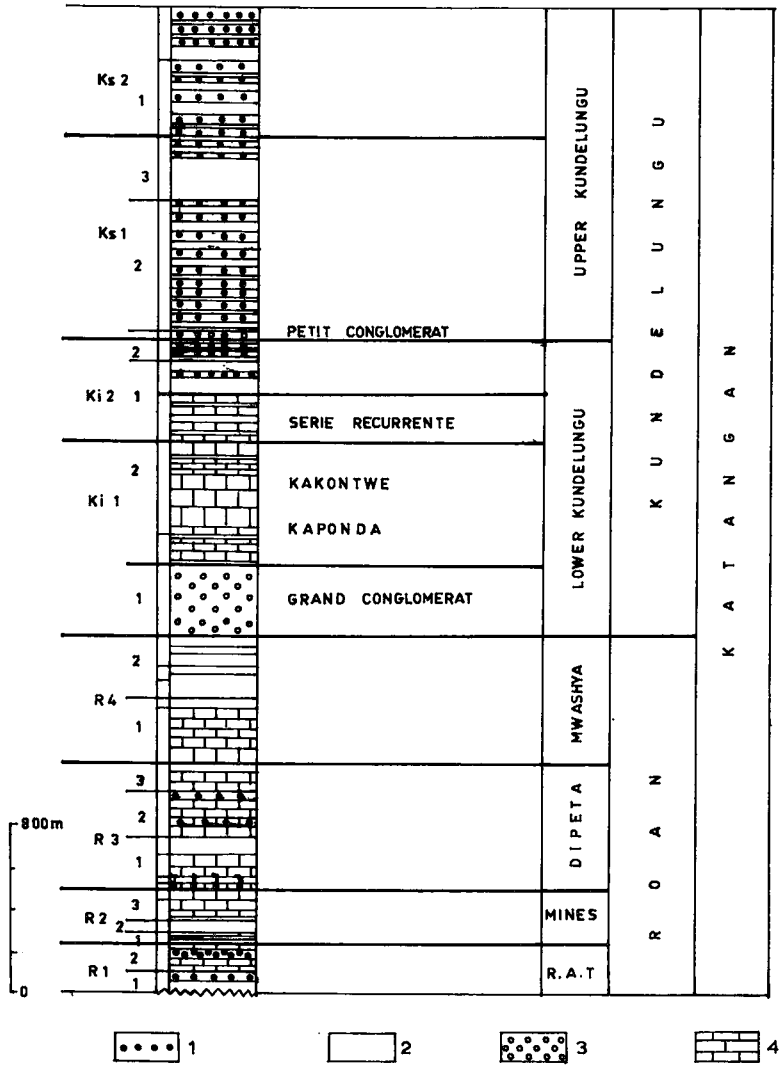

FIG. 2. Simplified stratigraphic column of the Katangan sediments in the Zairean sector of the Lufilian arc (Gecamines concession). The base is here unknown. Abbreviations: RAT clay–talc rocks; R Roan; Ki Lower Kundelungu; Ks Upper Kundelungu, 1 sandstone, 2 shale, 3 tillite, 4 dolomite. Modified after Intiomale (1982) and Lefebvre & Tshiauka (1986).

breccia body has been termed the Kipushi fault, and its central part defines the axial fault-zone (Intiomale & Oosterbosch 1974).

The axial fault breccia is composed of huge blocks of different lithologies derived from Roan Supergroup rocks. Blocks of a mafic green rock also are found in this breccia. The so-called Kipushi fault breccia, at the eastern margin of the breccia body, is perpendicular to the strike and contains rock fragments of the enclosing Lower Kundelungu beds. Their composition exclusively reflects strata in contact with the breccia or stratigraphically higher, suggesting that the breccia is a gravity-collapse feature. The breccia matrix is carbonaceous and exhibits sedimentary features (graded bedding, lamination) and structures indicative of collapse prior to folding of the enclosing host-rocks (Chabu 1990). De Magnée & François (1988) attributed the megabreccia in the cores of anticlines of the Zairean Copperbelt to evaporite

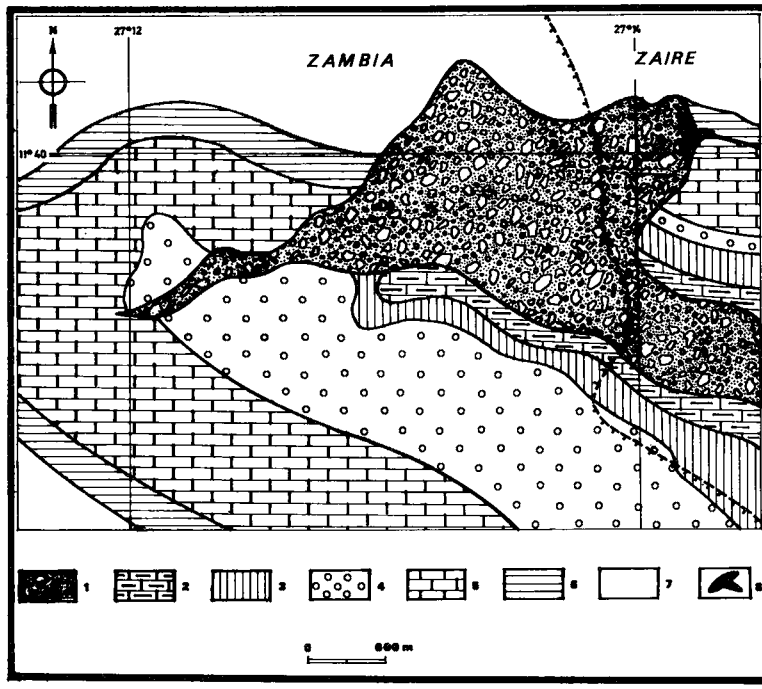

FIG. 3. Geological map of the Kipushi anticline and location of the orebody. 1 Breccia, 2 siliceous dolomite (Lower Mwashya), 3 shale (Upper Mwashya), 4 "Grand Conglomérat", 5 dolomite (Kakontwe), 6 shale and dolomite ("Série récurrente"), 7 shale and sandstone, 8 ore deposit. Modified after Intiomale (1982) and Gecamines Company records.

ascending diapirically under gravitational and tectonic stresses; the later dissolution of the salt formations resulted in collapse brecciation. However, the failure of hundreds of drill holes in the surrounding areas to intersect evaporite of sufficient thickness to explain the large ore-bearing breccias at Kipushi and several other Cu–Co deposits of the Zairean Copperbelt, lends no credence to this interpretation. Nor can it explain the formation of mineralized solution-cavities, some of which are discordant pipes found at Kipushi in unbrecciated Lower Kundelungu dolomites (see below).

The mineralization affected the base of the "Série récurrente", which is composed of alternating dolomites and dolomitic shales, and the karst structures in the underlying Kakontwe dolomites. Together with the rock matrix and gangue minerals, the ore also fills interfragmental voids of the collapse breccia described above. Remobilized ores also are common in veins.

Morphologically, the mineralization forms bodies that are either discordant or broadly concordant with lithological boundaries. The discordant bodies fill voids in collapse breccia and karstic structures that are mainly located in massive Middle to Lower Kakontwe dolomites. The concordant bodies are confined to well-bedded carbonaceous, black Upper Kakontwe dolomite and to the "Série récurrente", where the mineralization is predominantly cupriferous.

Important sulfide minerals are sphalerite, chalcopyrite, bornite, galena, pyrite, with minor tennantite, chalcocite, arsenopyrite, marcasite, renierite, briartite, gallite, germanite, betekhtinite and carrollite. The mineralization is zoned stratigraphically. Copper ores in the "Série récurrente" are separated from zinc–lead ores located in Middle to Lower Kakontwe dolomite stratigraphically below the copper ores. The transition zone between the two types of ores, which is found in the Upper Kakontwe, is a mixture of both types (Zn+Pb+Cu). All ore types are present in the collapse breccia.

Gangue minerals are phyllosilicates, feldspars, carbonates and quartz, with very rare barite. This study concentrates on barium-rich mica and feldspar. Other gangue minerals will be addressed in later studies.

MUSCOVITE

Muscovite and chlorite are the most abundant phyllosilicate minerals in the gangue. These appear in all ore types and are associated with all gangue minerals. Talc has not been observed within the mineralized zones, whereas phlogopite is minor.

Muscovite compositions include phengitic and barian varieties. Muscovite enriched in Ba was found in two mineral assemblages, at the 811 m and 992 m mine levels (depth): (i) Ba-bearing muscovite – Ba-bearing orthoclase – dolomite – barite – albite (+ rare hyalophane), and (ii) Ba-bearing muscovite – hyalophane – celsian – dolomite – barite – albite.

Ba-poor muscovite also is present in these unusual associations. It is generally finer grained than the Ba-rich muscovite. It should be noted that muscovite with as much as 3.06 wt.% BaO has been observed in the absence of barite and of (Ba,K)-feldspars.

Analyses of Ba-enriched muscovite were carried out at the Université Pierre et Marie Curie (Paris VI), using a Camebax Microbeam electron microprobe at an accelerating voltage of 15 kV, a beam current of 20 nA and a peak counting time of 15 seconds. The spot size was 1–2 μm. Standards used were natural and synthetic minerals or compounds, namely orthoclase for Si, Al and K, diopside for Mg and Ca, albite for Na, Fe_2O_3 for Fe, $MnTiO_3$ for Mn and Ti, sphalerite for Zn, barite for Ba, and LiF and fluorite for F. Results are given in Table 1.

TABLE 1. COMPOSITION OF BARIAN MUSCOVITE*

Analysis		1	2	3	4	5	6	7	8	9
SiO_2	wt.%	47.14	47.72	46.10	44.96	43.95	45.51	43.20	44.13	43.08
Al_2O_3		36.59	32.50	32.23	32.55	32.56	30.11	32.86	31.20	30.37
TiO_2		0.21	0.42	0.33	0.32	0.68	2.23	0.87	0.84	0.93
MnO		–	0.03	–	0.10	–	0.10	–	0.07	0.06
ZnO		–	0.04	0.02	–	0.07	0.07	0.01	0.52	0.03
FeO		0.29	0.22	0.42	0.02	0.08	0.11	0.06	0.12	0.02
MgO		2.49	2.57	2.40	2.04	2.03	2.34	1.82	2.16	2.04
CaO		–	–	–	–	–	0.06	–	–	–
BaO		3.73	3.63	4.34	5.41	5.78	6.30	6.76	7.51	5.41
Na_2O		0.26	0.27	0.31	0.42	0.36	0.19	0.36	0.30	0.42
K_2O		8.75	8.56	8.66	8.84	8.71	6.53	8.31	8.10	8.84
F		0.43	0.68	0.66	0.35	0.50	0.62	0.35	0.02	0.35
H_2O		4.25	4.18	4.08	4.18	4.06	4.02	4.11	4.27	4.18
F ≡ O		–0.18	–0.29	–0.28	–0.15	–0.21	–0.26	–0.15	–0.01	–0.15
Total		99.83	101.2	99.27	99.08	98.66	98.02	98.65	99.26	97.82
Formulas based on 24(O,OH,F)										
Si		6.34	6.35	6.29	6.21	6.13	6.32	6.06	6.19	6.16
^{IV}Al		1.66	1.65	1.71	1.79	1.87	1.68	1.94	1.81	1.84
^{VI}Al		3.50	3.49	3.48	3.51	3.47	3.25	3.38	3.35	3.28
Ti		0.04	0.04	0.03	0.04	0.07	0.24	0.09	0.09	0.10
Fe		0.03	0.02	0.05	–	0.01	0.01	0.01	0.01	0.03
Mg		0.50	0.51	0.49	0.42	0.42	0.48	0.48	0.45	0.47
Zn		–	–	–	–	0.01	0.01	–	0.05	0.09
Mn		–	–	–	0.01	–	0.01	–	–	–
Y		4.08	4.06	4.05	3.97	3.98	3.99	3.97	3.95	3.97
Ca		–	–	–	–	–	0.01	–	–	–
Ba		0.19	0.21	0.23	0.29	0.32	0.34	0.37	0.41	0.43
Na		0.07	0.06	0.08	0.11	0.10	0.05	0.10	0.08	0.08
K		1.47	1.48	1.51	1.56	1.55	1.16	1.49	1.45	1.43
X		1.73	1.75	1.82	1.96	1.97	1.56	1.96	1.94	1.94
F		0.18	0.29	0.28	0.15	0.22	0.27	0.15	0.01	0.15

A dash represents a concentration less than the detection limit of the electron microprobe and less than 0.001 atoms per formula unit. * Electron-microprobe data.

BaO contents range from 3.63 to 7.66 wt.%, with 6 wt.% BaO being more common in muscovite from both of the above mineral assemblages. Similar values have been reported in muscovite from a stratabound Ba–Zn mineralization subjected to amphibolite-grade regional metamorphism at Aberfeldy, Scotland (Fortey & Beddoe-Stephens 1982). Pan & Fleet (1991) also reported on muscovite with up to 10.3 wt.% BaO in the Hemlo area, Ontario. The barium content is rarely constant, even within individual grains. The following discussion of the compositional variations in muscovite emphasizes the nature of coupled substitutions involved to achieve charge balance.

Examination of Table 1 shows that occupancy of the octahedral sites ranges between 3.95 and 4.08. Octahedrally coordinated Al occupies 87% of the total occupied positions, the remaining being mostly Mg and Fe. Titanium contents are relatively high, ranging from 0.02 to 0.24 ions per formula unit, whereas Mn and Zn are generally below the detection limits.

Si is commonly greater than 6 atoms per formula unit; in comparison, the associated Ba-poor muscovite (data not included) have still higher contents of Si and Mg. The total occupancy of the interlayer site ranges from 1.56 to 1.98, including 1.16 to 1.56 K and 0.19 to 0.43 Ba per formula unit. These barium contents in muscovite are comparable to those reported by Fortey & Beddoe-Stephens (1982) and by Dymek *et al.* (1984). The low occupancy of some of the interlayer sites may be due to vacancies resulting from a 1:1 replacement of K^+ by Ba^{2+} in the substitution scheme Ba + N = 2K (Guidotti 1984). However, the lack of a negative correlation between the Ba contents and the total number of interlayer cations indicates that this model of substitution is not the most effective. Ba and Ti contents are positively correlated (Fig. 4). Pan & Fleet (1991) also reported high Ti contents in barian muscovite.

There is a crude negative correlation between Ba contents and the total number of octahedrally coordinated cations (Fig. 5), which suggests that the excess interlayer charge is partly balanced by increasing vacancies in the octahedral site, resulting in an increase in negative charge in the layer of octahedra. This relationship may be due to the positive correlation of Ba with Ti shown in Figure 4; however, on a plot of Ti *versus* total octahedrally coordinated cations, the data are more scattered than in the above relationship (Fig. 5). This fact casts doubt on the existence of the substitution $2^{VI}R^{2+} = {}^{VI}Ti + N$, reported by Guidotti (1984) in both biotite and muscovite, as a possible scheme for the incorporation of Ti in the muscovite analyzed, thus indicating that the relationship between Ba and the total number of octahedral cations is not due to Ti.

Si displays a relatively well-defined negative correla-

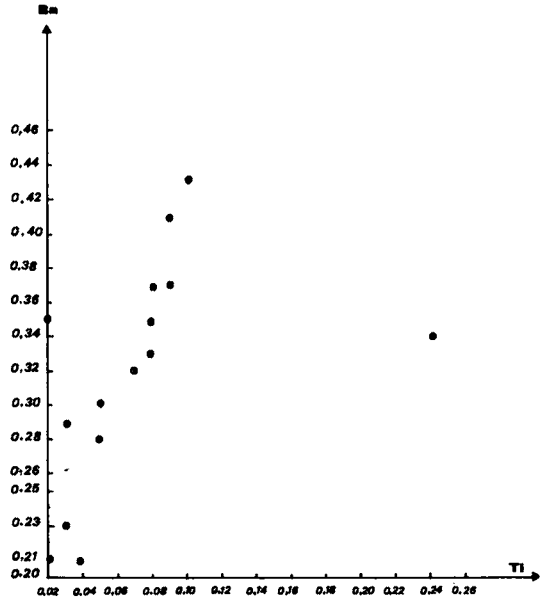

FIG. 4. Relationship between Ti and Ba in barian muscovite.

tion with Al (Fig. 6A). This is an expression of the common phengitic substitution of normal muscovite $(Mg,Fe)^{2+}Si = {}^{VI}Al^{IV}Al$. If the muscovite is a binary

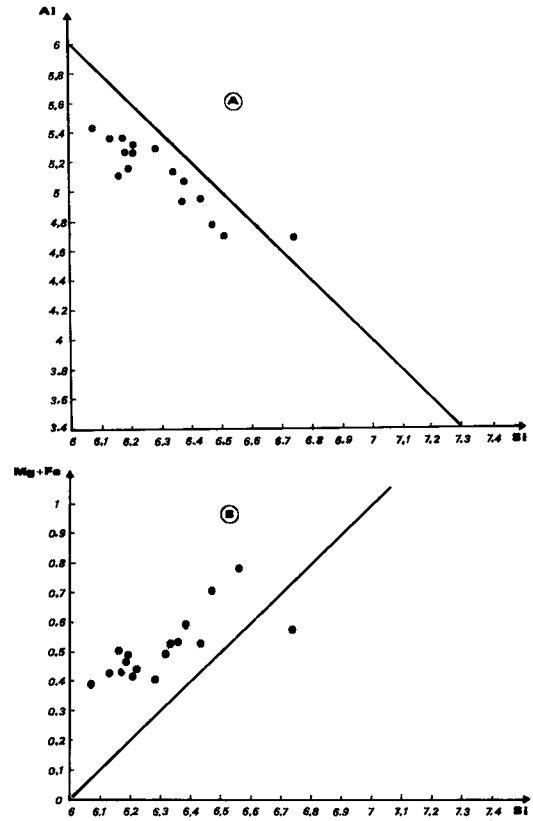

FIG. 6. A. Relationship between Al and Si in muscovite (phengitic substitution). B. Relationship between Mg+Fe and Si expressing the Tschermak or phengitic substitution.

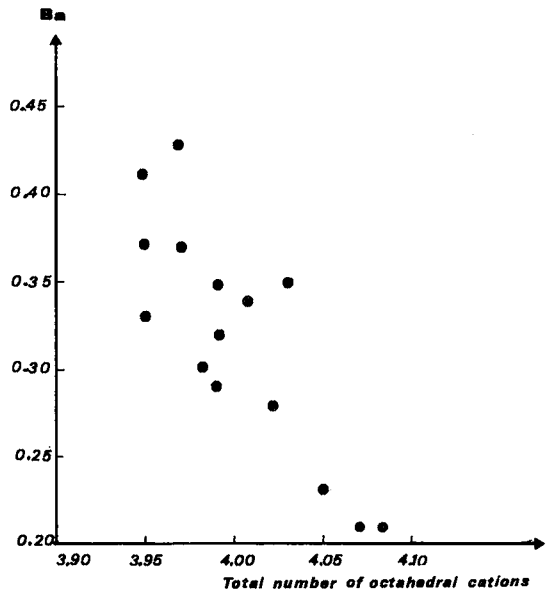

FIG. 5. Variation of the occupancy of octahedrally coordinated sites with Ba content in muscovite.

solid-solution composed of end-member muscovite and celadonite (Guidotti 1984, Miyashiro & Shido 1985) by Tschermak substitution, it must plot on the straight line shown in the diagrams (Fig. 6). Actually, most compositions plot considerably below the straight line in Figure 6A and considerably above the ideal slope in Figure 6B. The Al content (too low) and the (Mg+Fe) content (too high) result from the fact that Al also is involved in other substitutions, such as $Ti = {}^{VI}Al$ (Guidotti 1984) and BaAl = (Na,K)Si (Fortey & Beddoe-Stephens 1982, Guidotti 1984), as depicted in Figure 7. Despite a considerable scatter in the data, Figure 7 shows a broad positive correlation between Ba and ^{IV}Al. The excess interlayer charge resulting from the replacement of K by Ba thus seems also partly balanced by substitution of Al for Si in tetrahedral positions.

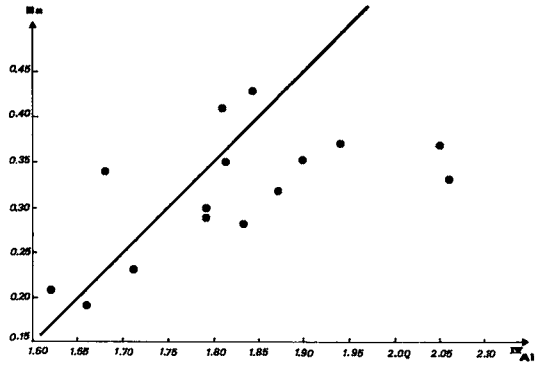

FIG. 7. Correlation of Ba with ^{IV}Al in muscovite. The two compositions of Ba-rich muscovite showing the highest ^{IV}Al contents deviate from a muscovite composition in that they have less than 6 Si atoms per formula unit (Guidotti 1984). These could then be neglected in interpretations of this diagram.

(Ba,K)-FELDSPARS

In the Kipushi deposit, the (Ba,K)-feldspars include orthoclase, hyalophane and celsian. These represent about 1% in volume of some ores and are confined to the same mineral assemblages as barian muscovite. These feldspars mostly occur as optically inhomogeneous untwinned crystals in which cleavage is generally poorly developed. Celsian and hyalophane commonly display sector zoning and complex patterns of extinction. They show white-grey, turbid and dark grey zones in crossed nicols. These zones, of variable width and habit, bear different chemical compositions, the clear zones being richer in barium than darker zones. These probably represent unmixed crystals. Orthoclase grains also show undulatory extinction, but they have a constant composition. The nearly euhedral rhombic grains of orthoclase are enclosed in dolomite and sphalerite.

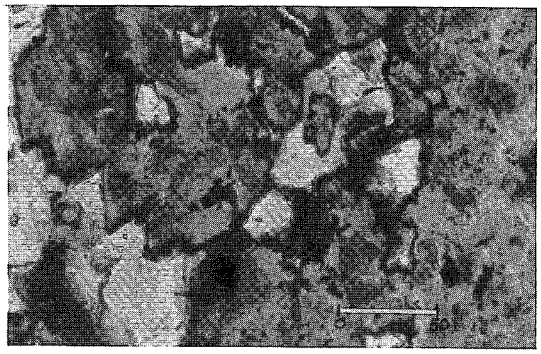

FIG. 8. Photomicrograph showing relict grains of barite (white) in orthoclase. Scale bar: 50 μm.

Locally, the orthoclase encloses relict barite (Fig. 8) and is commonly corroded by dolomite.

Results of electron-microprobe analyses of the (Ba,K)-feldspar grains, at instrumental conditions described above, are given in Table 2. In terms of a Cn–Or–Ab diagram (Fig. 9), the (Ba,K)-feldspars from Kipushi can be divided into three types: (i) Cn-rich specimens with compositions $Cn_{56-84}Or_{13-39}Ab_{3-4}$, (ii) Cn-poor, Or-rich feldspars with the compositions $Cn_{1-5}Or_{93-99}Ab_{0-1}$, which show very low contents of albite, and (iii) specimens with intermediate compositions: $Cn_{31-0}Or_{41-51}Ab_{8-11}$. One feldspar of this type has an inclusion of an albite-rich phase, probably representing an unmixed crystal with the composition $Cn_4Or_{20}Ab_{76}$.

It is noteworthy that the albite content of these feldspars increases from the orthoclase end-member toward Ba-poor hyalophane, whereas it decreases from Ba-poor hyalophane to Ba-rich hyalophane (Cn_{56-63}). Ba-rich hyalophane and celsian have the same amount (3–4 mole % Ab) of albite content. There is a greater spread in the albite content (1–5%) of celsian from the zone of Ba–Zn mineralization in the Scottish Dalradian (Fortey & Beddoe-Stephens 1982). Viswanathan & Kielhorn (1983) reported a decrease in the albite content with an increase in Cn content in Ba-rich feldspar from Otjosondu, Namibia. In their study, the albite content of a barian feldspar containing 30–40% celsian is higher (more than 20 mole % Ab) than in feldspar with 46–55%

TABLE 2. CHEMICAL COMPOSITION OF (Ba,K)-FELDSPAR*

Analysis	1	2	3	4	5		6	7	8	9
SiO_2	wt.%	64.30	64.20	62.04	64.35	53.18	49.75	44.57	40.00	37.65
Al_2O_3		18.95	19.42	19.06	18.86	22.07	24.13	25.30	26.81	27.75
TiO_2		–	–	0.01	0.02	–	0.02	0.05	0.05	–
MnO		–	0.12	–	0.05	–	–	–	–	–
ZnO		0.05	–	–	0.03	0.11	0.18	0.04	0.11	0.07
FeO		0.07	–	0.12	–	–	–	0.05	–	0.08
MgO		–	0.01	–	0.02	–	–	–	–	0.01
CaO		–	–	0.05	0.09	0.03	–	–	0.01	–
BaO		0.83	1.66	2.83	2.98	14.67	18.72	26.07	31.99	35.00
Na_2O		0.11	0.10	0.03	0.06	0.97	1.00	0.47	0.34	0.28
K_2O		15.70	15.41	15.20	14.60	8.66	6.81	4.14	2.62	1.68
Total		100.02	100.9	99.29	101.05	99.78	100.61	100.84	101.93	102.58
Formulas based on 8 atoms of oxygen										
Si		2.98	2.96	2.94	2.98	2.70	2.57	2.42	2.85	2.16
Al		1.03	1.06	1.06	1.03	1.32	1.47	1.62	1.78	1.87
Ti		–	–	–	0.001	–	0.001	0.002	0.002	
Fe		0.003	–	0.005	–	–	–	0.002	–	0.004
Mg		–	0.001	–	0.001	–	–	–	–	0.001
Zn		0.002	–	–	0.001	0.004	0.007	0.002	0.005	0.003
Mn		–	0.005	–	0.002	–	–	–	–	–
Ca		–	–	0.003	0.005	0.002	–	–	0.001	–
Ba		0.02	0.03	0.05	0.05	0.29	0.38	0.55	0.71	0.79
Na		0.01	0.01	0.003	0.005	0.10	0.10	0.05	0.04	0.03
K		0.93	0.91	0.92	0.86	0.56	0.45	0.29	0.19	0.12
Molecular proportions (%)										
Cn		2.1	3.2	5.1	5.5	30.5	40.9	61.8	75.5	84.0
Ab		1.0	1.1	0.3	0.6	10.5	10.7	5.6	4.3	3.2
Or		96.9	95.7	94.6	93.9	59.0	48.4	32.6	20.2	12.8

A dash represents a concentration less than the detection limit of the electron microprobe and less than 0.001 atoms per formula unit. * Electron-microprobe data.

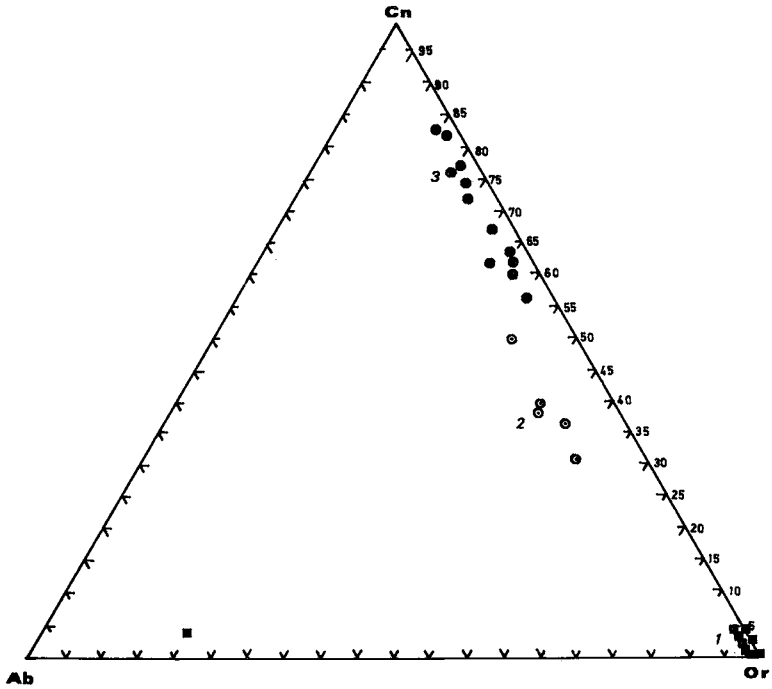

FIG. 9. Variations in chemical composition of the (Ba,K)-feldspars from Kipushi, Zaire. 1 Cn-poor specimens, 2 feldspar with intermediate composition, 3 Cn-rich feldspar.

celsian (10–12% Ab). In the present study, there is no change in the albite content of feldspars (8–11% Ab) over this compositional range. However, a strong decrease in the albite content does appear in Ba-rich feldspar containing at least 56% celsian.

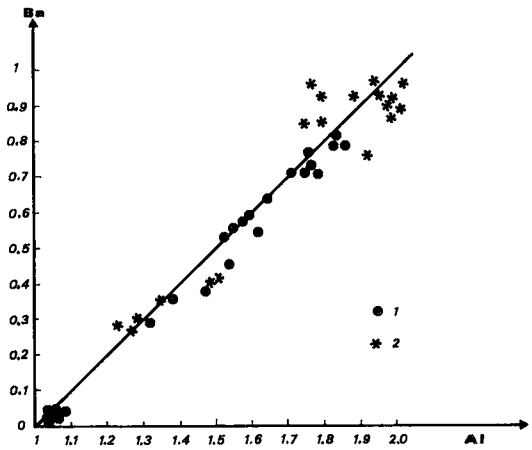

FIG. 10. Correlation of Ba with Al in (Ba,K)-feldspar. Line represents theoretical substitution. 1 Data from this study, 2 additional data from Fortey & Beddoe-Stephens (1982).

Examination of Figure 9 suggests the presence of two compositional discontinuities, at Cn_{5-30} and Cn_{40-50}. Pan & Fleet (1991) also reported a compositional discontinuity at Cn_{15-25} and two more at Cn_{30-40} and Cn_{47-65}, whereas Gay & Roy (1968) postulated a compositional gap between Cn_{65} and Cn_{80}, also reported by Fortey & Beddoe-Stephens (1982); in the present study, the composition of (Ba,K)-feldspars is continuous through this compositional range.

The feldspar compositions plot close to the ideal line BaAl = (Na,K)Si (Fig. 10) in the series $KAlSi_3O_8$ – $BaAl_2Si_2O_8$, reflecting the low abundance of other cations in the feldspar structure as compared to muscovite. But most of our data plot slightly below the line, especially in those cases representing feldspar with relatively high albite contents.

DISCUSSION

The Katangan episode of regional metamorphism (650–500 Ma) has affected the Kipushi deposit (Chabu 1990). It is of lower greenschist facies and is characterized by the following mineral assemblages: (i) dolomite – albite – muscovite – quartz – biotite (phlogopite) – chlorite in ores, and (ii) dolomite – quartz – albite – talc – magnesite – phlogopite in gypsum- and anhydrite-

bearing dolomite in the "Série récurrente", above the mineralization.

These mineral assemblages give support to the suggestion by Lefebvre & Patterson (1988) that the Kipushi deposit is situated in the biotite zone of the regionally metamorphosed sequence.

Available experimental data (Winkler 1965, 1967, Puhan & Johannes 1974) and studies of metamorphosed carbonate rocks (Ferry 1976, Rice 1977, Bowman & Essene 1982) are consistent with the first development of biotite under a total pressure of a few kilobars, at temperatures between 300° and 400°C.

The biotite – chlorite isograd reaction muscovite + dolomite + quartz + water = biotite + chlorite + calcite + carbon dioxide, which seems to apply to the mineral assemblages found in the Kipushi deposit, was estimated to occur at 370°C in the metamorphism of impure dolomite (Ferry 1976).

Experiments (Fawcett & Yoder 1966) indicate that Mg-rich chlorite is stable over a wider range of P–T conditions than Fe-rich chlorite. The stability field of the latter is drastically limited under reducing conditions to a temperature below 350°C under a pressure of 1 kbar. Since Fe-rich chlorite is present in the reducing environment of the Kipushi ores (Chabu 1990), it seems reasonable to assume that the temperature that affected the deposit during the Katangan regional metamorphism was below 350°C. This is in agreement with Cluzel's (1986) estimate of the P–T conditions of the Katangan regional metamorphism in the area.

Conclusions

Although barian feldspar is most common in manganese deposits (Deer *et al.* 1962, 1963), celsian also has been reported in cases of exhalative base-metal mineralization (Fortey & Beddoe-Stephens 1982). These authors suggested that Ba-rich feldspar and barian muscovite in the schists at the Aberfeldy Ba–Zn deposit, Scotland, originated either by replacement of barite or by the dehydration of cymrite [$BaAl_2Si_2(O,OH)_8 \cdot H_2O$] during metamorphism. Pan & Fleet (1991) also concluded that barian muscovite and (Ba,K)-feldspar in the late Archean Hemlo – Hero Bay greenstone belt, Ontario, were formed by regional thermal metamorphism of a barite-rich unit.

The close association of barian silicates with barite-bearing metamorphic mineral assemblages and the presence of relict barite in some Ba-bearing orthoclase grains give support to the suggestion that barian muscovite and (Ba,K)-feldspar in the Kipushi deposit derived their barium by the breakdown of barite during Katangan metamorphism.

Under oxidizing conditions, barite is stable up to very high temperature (*e.g.*, 1000°C: Segnit & Gelb 1970). This fact accounts for its survival in some high-grade amphibolite-facies metamorphic rocks (Fortey & Beddoe-Stephens 1982). For barian silicates to form from barite, a reducing agent is necessary. This has been demonstrated in experiments in ceramic systems (Segnit & Gelb 1970). Heating of kaolinite–barite mixtures up to 1000°C failed to produce any barian silicates, but when carbon was added to the mixture, the sulfate was reduced according to the following reaction:

$$BaSO_4 + 4C \rightarrow BaS + 4CO$$

$$3BaSO_4 + BaS \rightarrow 4BaO + 4SO_2$$

and celsian was formed at 800°C. To form celsian from barium carbonate and kaolinite, a reducing agent was naturally not necessary. Although these experiments were carried out at a much higher temperature than that which can be expected to apply to assemblages of metamorphic minerals found at Kipushi, they show that in the absence of a reducing agent, barite is stable at a temperature at which barian feldspar may form in its presence.

Because of the very low solubility of barite (Blount 1977) and considering the fact that this mineral is unstable under sulfate-reducing conditions or conditions that favor the formation of witherite, $BaCO_3$ (Segnit & Gelb 1970, Blount 1977), we assume that for barian muscovite and (Ba,K)-feldspar to have formed in the Kipushi deposit, barite was first decomposed by reaction with either CO produced during the metamorphism of impure dolomite or with carbonaceous matter. The latter is abundant in the Kakontwe dolomite (see above) and in karstic structures (Chabu 1990). The released BaO reacted with quartz, detritic or diagenetic chlorite or clay minerals to form barian silicates during the Katangan regional metamorphism.

Acknowledgements

The authors express their deep gratitude to D. Velde, Université Paris VI, and B. Velde, Ecole Normale Supérieure, Paris, for helpful discussions during the preparation of the manuscript. Constructive comments from two reviewers and R.F. Martin have helped to improve the quality of this paper.

References

Blount, C.W. (1977): Barite solubilities and thermodynamic quantities up to 300°C and 1400 bars. *Am. Mineral.* **62**, 942-957.

Bowman, J.R. & Essene, E.J. (1982): P–T–X(CO_2) conditions of contact metamorphism in the Black Butte aureole, Elkhorn, Montana. *Am. J. Sci.* **282**, 311-340.

Chabu, M., (1990): Metamorphism of the Kipushi carbonate hosted Zn–Pb–Cu deposit (Shaba, Zaire). *In* Regional Metamorphism of Ore Deposits and Genetic Implications (P.G. Spry & L.T. Bryndzia, eds.). VSP, Utrecht, Holland (27-47).

Cluzel, D. (1986): Contribution à l'étude du métamorphisme des gisements cupro-cobaltifères stratiformes du Sud-Sha-

ba, Zaïre. Le district minier de Lwisha. *J. Afr. Earth Sci.* **5**, 557-574.

DEER, W.A., HOWIE, R.A. & ZUSSMAN, J. (1962): *Rock-Forming Minerals.* **3**. *Sheet Silicates.* Longmans, London.

_____, _____ & _____ (1963): *Rock-Forming Minerals.* **4**. *Framework Silicates.* Longmans, London.

DYMEK, R.F., BOAK, J.L. & KERR, M.J. (1983): Green micas in the Archean Isua and Malene supracrustal rocks, southern western Geenland, and the occurrence of barian–chromian muscovite. *Rapp. Grønlands Geol. Unders.* **112**, 71-82.

FAWCETT, J. & YODER, H.S., JR. (1966): Phase relationships of chlorites in the system MgO–Al_2O_3–SiO_2–H_2O. *Am. Mineral.* **51**, 353-380.

FERRY, J.M. (1976): Metamorphism of calcareous sediments in the Waterville–Vassalboro area, south central Maine: mineral reactions and graphical analysis. *Am. J. Sci.* **276**, 841-882.

FORTEY, N.J. & BEDDOE-STEPHENS, B. (1982): Barium silicates in stratabound Ba–Zn mineralization in the Scottish Dalradian. *Mineral. Mag.* **46**, 63-72.

GAY, P. & ROY, N.N. (1968): The mineralogy of the potassium–barium feldspar series. III. Subsolidus relationships. *Mineral. Mag.* **36**, 914-932.

GUIDOTTI, C.V. (1984): Micas in metamorphic rocks. *In* Micas (S.W.Bailey, ed.). *Rev. Mineral.* **13**, 357-467.

INTIOMALE, M.M. (1982): *Le gisement Zn–Pb–Cu de Kipushi. Étude géologique et métallogénique.* Thèse de doctorat, Univ. Catholique de Louvain, Louvain-la-Neuve, Belgique.

_____ & OOSTERBOSCH, R. (1974): Geologie et géochimie du gisement de Kipushi, Zaïre. *In* Gisements stratiformes et provinces cuprifères (P. Bartholomé, ed.). Société Géologique de Belgique, Liège, Belgique (123-164).

LEFEBVRE, J.J. & PATTERSON, L.E. (1982): Hydrothermal assemblages of aluminium serpentine, florencite and kyanite in the Zairean Copperbelt. *Soc. Géol. Belg., Annales* **105**, 51-71.

_____ & TSHIAUKA, T. (1986): Le groupe des mines à Lubembe (Shaba, Zaïre). *Soc. Géol. Belg., Annales* **109**, 557-571.

DE MAGNÉE, I. & FRANÇOIS, A. (1988): The origin of the Kipushi (Cu,Zn,Pb) deposit in direct relation with a Proterozoic salt diapir, Copperbelt of Central Africa, Shaba, Republic of Zaire. *In* Base Metal Sulfide Deposits (G.H. Friedrich & P.M. Herzig, eds.). Springer Verlag, Berlin (74-93).

MIYASHIRO, A. & SHIDO, F. (1985): Tschermak substitution in low- and middle-grade pelitic schists. *J. Petrol.* **26**, 449-487.

PAN, YUANMING & FLEET, M.E. (1991): Barian feldspar and barian–chromian muscovite from the Hemlo area, Ontario. *Can. Mineral.* **29**, 481-498.

PUHAN, D. & JOHANNES, W. (1974): Experimentelle Untersuchung der Reaktion Dolomit + Kalifeldspat + H_2O ⇋ Phlogopit + Calcit + CO_2: ein Methodenvergleich. *Contrib. Mineral. Petrol.* **48**, 23-31.

RICE, J.M. (1977): Progressive metamorphism of impure dolomitic limestone in the Marysville aureole, Montana. *Am. J. Sci.* **277**, 1-24.

SEGNIT, E.R. & GELB, T. (1970): Reactions of kaolinite with barium carbonate and barium sulphate. *Aust. J. Ceram. Soc.* **6**, 12-18.

VISWANATHAN, K. & KIELHORN, H.M. (1983): Variations in the chemical compositions and lattice dimensions of (Ba,K,Na)-feldspars from Otjosondu, Namibia, and their significance. *Am. Mineral.* **68**, 112-121.

WINKLER, H.G.F. (1965): *Die Genese der metamorphen Gesteine.* Springer-Verlag, Berlin.

_____ (1967): *Petrogenesis of Metarmorphic Rocks* (2nd ed.). Springer-Verlag, Berlin.

Received October 11, 1991, revised manuscript accepted February 1, 1992.